

Physicochemical Characterization, Development and Evaluation of Curcumin-Loaded Nanoparticles for Antiproliferative, Activity against Pancreatic Cancer (PANC-1) Cells

¹M. Sivakumar*, ²Preeti Mangala, ³Palash Chandra Biswas, ⁴Mohit Kumar, ⁵Abdul Kadir Jilani, ⁶Sunil Sugnomal Menghani, ⁷Jyothi Basini, ⁸R. Gopinath

¹Professor, Department of Pharmacognosy, Faculty of Pharmacy, Sree Balaji Medical College and Hospital, BIHER (DU), Chromepet, Chennai, Tamil Nadu. 600044

EMail- sivakumar.pharm@bharathuniv.ac.in

²Associate Professor and Head, Department of Chemistry, Jyoti Nivas College Autonomous, Koramangala, Hosur Road, Bangalore - 560 095, Karnataka.

Email:- preeti.mangala@gmail.com

³Assistant Professor, Netaji Subhas Chandra Bose Institute of Pharmacy, Chakdaha - Bongaon Rd, Roypara, Tatla, West Bengal, 741222

Email:-palashbiswas76@yahoo.com

⁴Assistant professor, Teerthanker Mahaveer College of Pharmacy, Teerthanker Mahaveer University, Moradabad, Uttar Pradesh. mohitgoyal21111@gmail.com

ORCID ID:-0009-0001-8236-7396

⁵Assistant Professor, School of Pharmaceutical Sciences, University of Science and Technology Meghalaya, Ri-Bhoi, Techno City, Killing Road, Baridua, Meghalaya. 793101 Email: salikadi16@gmail.com

⁶Principal, Gondia College of Pharmacy, Gondia, Maharashtra. 441601

sunil sunmegh@rediffmail.com

⁷Professor and HOD, Seven Hills College of Pharmacy (Autonomous), Tirupati, Andhra Pradesh, India. 517561 Email:jyothi 811@yahoo.co.in

⁸PG scholar, Seven Hills College of Pharmacy (Autonomous), Tirupati, Andhra Pradesh, India. 517561 Email:-

gopinath143524@gmail.com

Corresponding Authors

¹M. Sivakumar*

¹Professor, Department of Pharmacognosy, Faculty of Pharmacy, Sree Balaji Medical College and Hospital, BIHER (DU), Chromepet, Chennai, Tamil Nadu. 600044 EMail- sivakumar.pharm@bharathuniv.ac.in

ABSTRACT

Background: Pancreatic cancer is one of the most aggressive malignancies, associated with poor prognosis and limited therapeutic options. Curcumin, a bioactive polyphenolic compound from Curcuma longa, exhibits strong anticancer properties but is hindered by poor solubility and low bioavailability. Nanoparticle-based delivery systems can potentially overcome these challenges and enhance therapeutic efficacy.

Methods: Curcumin-loaded nanoparticles were prepared using the nanoprecipitation method and optimized through a Box–Behnken design. The formulations were characterized for particle size, polydispersity index (PDI), zeta potential, morphology, encapsulation efficiency, and thermal behavior. In vitro drug release was assessed using the dialysis bag method. Antiproliferative activity against PANC-1 cells was evaluated through MTT assay, Annexin V–FITC/PI apoptosis assay, and cell cycle analysis. Stability studies were conducted on lyophilized nanoparticles under refrigerated storage for three months.

Results: The optimized formulation displayed a mean particle size of 142.3 ± 5.6 nm, PDI of 0.212 ± 0.02 , zeta potential of -24.7 ± 2.1 mV, and encapsulation efficiency of $89.2 \pm 3.5\%$. Drug release was sustained up to 72 h with 86.2% cumulative release. Compared with free curcumin, nanoparticles demonstrated a 3.5-fold lower IC50, significantly enhanced apoptosis, and G2/M phase arrest.

Conclusion: Curcumin-loaded nanoparticles improved solubility, stability, and antiproliferative activity against PANC-1 cells, highlighting their potential as an effective therapeutic strategy for pancreatic cancer.

KEYWORDS: Curcumin, nanoparticles, pancreatic cancer, PANC-1, apoptosis, cell cycle arrest.

How to Cite: M. Sivakumar, Preeti Mangala, Palash Chandra Biswas, Mohit Kumar, Abdul Kadir Jilani, Sunil Sugnomal Menghani, Jyothi Basini, R. Gopinath, (2025) Physicochemical Characterization, Development and Evaluation of Curcumin-Loaded Nanoparticles for Antiproliferative, Activity against Pancreatic Cancer (PANC-1) Cells, Vascular and Endovascular Review, Vol.8, No.8s, 261-273.

INTRODUCTION

Pancreatic cancer is among the most lethal malignancies, characterized by aggressive progression, late diagnosis, and poor prognosis. It currently ranks as the seventh leading cause of cancer-related mortality worldwide and carries a five-year survival rate of less than 10% (Siegel et al., 2023). The poor survival outcomes are largely attributed to the asymptomatic nature of early disease, limited effectiveness of screening modalities, and resistance to conventional therapies. Standard treatment options such as surgery, radiation, and systemic chemotherapy offer only modest survival benefits. Chemotherapeutic regimens including gemcitabine or combinations such as FOLFIRINOX have improved patient outcomes slightly, but these are often associated with systemic toxicity, multidrug resistance, and minimal long-term efficacy (Springfeld et al., 2019). Consequently, there is an urgent need for safer and more effective therapeutic strategies that can overcome the intrinsic challenges of treating pancreatic tumors. Curcumin, a yellow polyphenolic compound derived from the rhizome of Curcuma longa (turmeric), has attracted significant attention due to its diverse pharmacological activities. Numerous studies have demonstrated its anti-inflammatory, antioxidant, and anticancer properties, mediated by modulation of key molecular pathways such as NF-κB, STAT3, PI3K/Akt, and MAPK (Kunnumakkara et al., 2017). In cancer models, curcumin has been shown to induce apoptosis, inhibit angiogenesis, and suppress metastasis. Specifically in pancreatic cancer, curcumin has demonstrated the ability to sensitize tumor cells to chemotherapeutic agents such as gemcitabine, suggesting its potential as a complementary therapy (Bao et al., 2013). Despite its promising pharmacological profile, clinical translation of curcumin has been severely hindered by its poor aqueous solubility (<0.1 mg/mL), instability at physiological pH, rapid systemic metabolism, and poor oral bioavailability (Anand et al., 2007). These limitations result in subtherapeutic plasma concentrations, preventing curcumin from exerting meaningful anticancer effects in vivo. Conventional formulations such as suspensions and capsules have failed to address these challenges, highlighting the necessity for advanced delivery systems that can improve curcumin's stability, solubility, and targeted delivery to tumor tissues.

Nanoparticle-based drug delivery systems offer a promising approach to overcome these barriers. Polymeric nanoparticles, particularly those composed of biodegradable polymers such as PLGA, provide controlled drug release, high encapsulation efficiency, and enhanced accumulation in tumors through the enhanced permeability and retention (EPR) effect (Danhier et al., 2012). Several preclinical studies have demonstrated that curcumin-loaded nanoparticles exhibit enhanced cytotoxicity and bioavailability compared to free curcumin, validating this strategy as a potential therapeutic modality (Mukerjee & Vishwanatha, 2009).

In light of these considerations, the present study was designed to formulate and optimize curcumin-loaded nanoparticles using a systematic experimental design approach. The physicochemical properties of the nanoparticles, including particle size, surface charge, encapsulation efficiency, and release behaviour, were evaluated. Furthermore, the antiproliferative activity of the optimized formulation was assessed in vitro against human pancreatic carcinoma (PANC-1) cells through cytotoxicity, apoptosis, and cell cycle studies. The objective was to determine whether nanoparticle encapsulation could enhance curcumin's therapeutic potential against pancreatic cancer and lay the groundwork for future translational studies.

MATERIALS AND METHODS

2.1 Materials

Curcumin of analytical grade (>95% purity) was procured from Sigma-Aldrich (St. Louis, MO, USA). Poly(lactic-co-glycolic acid) (PLGA, 50:50, inherent viscosity 0.55–0.75 dL/g) was purchased from Evonik Industries (Germany) and used as the primary biodegradable polymer matrix. Polyvinyl alcohol (PVA; molecular weight 30,000–70,000, 87–89% hydrolyzed) served as the stabilizer and was purchased from Merck (Darmstadt, Germany). Acetone, ethanol, and phosphate-buffered saline (PBS, pH 7.4) were of analytical grade and obtained from HiMedia (Mumbai, India). Dialysis tubing with a molecular weight cut-off (MWCO) of 12–14 kDa was purchased from Spectrum Labs (USA). The human pancreatic carcinoma cell line PANC-1 was obtained from the American Type Culture Collection (ATCC, Manassas, VA, USA). Dulbecco's Modified Eagle Medium (DMEM), fetal bovine serum (FBS), penicillin-streptomycin, and trypsin-EDTA were purchased from Gibco (Thermo Fisher Scientific, Waltham, MA, USA). Annexin V–FITC apoptosis detection kits and propidium iodide (PI) were purchased from BD Biosciences (San Jose, CA, USA). All other reagents used were of analytical grade and used without further purification.

2.2 Preparation of Curcumin-Loaded Nanoparticles

Curcumin-loaded nanoparticles were prepared using the nanoprecipitation method, a solvent displacement technique chosen for its reproducibility and ability to produce nanoscale particles with high entrapment efficiency. In brief, accurately weighed amounts of PLGA and curcumin were dissolved in 10 mL of acetone to prepare the organic phase. The ratio of curcumin to polymer was varied according to the experimental design, ranging from 1:5 to 1:15. The organic phase was then added dropwise to 50 mL of an aqueous phase containing PVA as a stabilizer, maintained under magnetic stirring at 800 rpm. The addition was controlled using a syringe pump at a flow rate of 1 mL/min to ensure controlled mixing and prevent particle aggregation. The resultant colloidal suspension was stirred for 4 h at room temperature to allow complete solvent evaporation. Nanoparticles were collected by centrifugation at 15,000 rpm for 30 min at 4°C (Eppendorf 5804R, Germany). The pellet obtained was washed three times with Milli-Q water to remove excess stabilizer and unencapsulated drug. Finally, the washed suspension was lyophilized using a Christ Alpha 1–2 LD Plus freeze-dryer (Germany) to obtain free-flowing powder, which was stored at 4°C until further use.

2.3 Experimental Design and Optimization

A three-factor, three-level Box—Behnken design (BBD) was employed to optimize the nanoparticle formulation. The independent variables selected were polymer concentration (X1: 50–150 mg), drug-to-polymer ratio (X2: 1:5–1:15), and PVA stabilizer concentration (X3: 0.5–2%). The dependent responses were particle size (Y1), polydispersity index (Y2), and encapsulation

efficiency (Y3). A total of 17 experimental runs were generated by Design-Expert software version 13 (Stat-Ease Inc., Minneapolis, USA), including five center points to evaluate reproducibility. All formulations were prepared in triplicate, and experimental values were compared with predicted values to validate the model. Desirability function analysis was employed to identify the optimum formulation parameters that minimized particle size and PDI while maximizing encapsulation efficiency.

2.4 Characterization of Nanoparticles

2.4.1 Particle Size, Polydispersity, and Zeta Potential

Dynamic light scattering (DLS) was employed to measure the mean particle size, polydispersity index (PDI), and zeta potential using a Malvern Zetasizer Nano ZS90 (Malvern Instruments, UK). Samples were diluted tenfold with deionized water to avoid multiple scattering effects and analyzed at 25° C with a scattering angle of 90° . All measurements were performed in triplicate, and results were expressed as mean \pm standard deviation (SD).

2.4.2 Morphological Analysis

Surface morphology and shape of nanoparticles were examined using scanning electron microscopy (SEM, JEOL JSM-IT300, Japan). Lyophilized nanoparticles were mounted on aluminum stubs, coated with a thin layer of gold using a sputter coater, and visualized at an accelerating voltage of 15 kV. Selected samples were also imaged using transmission electron microscopy (TEM, FEI Tecnai G2, USA) for internal structure evaluation.

2.4.3 Encapsulation Efficiency and Drug Loading

Encapsulation efficiency (EE%) and drug loading (DL%) were determined by dissolving an accurately weighed quantity of lyophilized nanoparticles in acetone to release curcumin. The solution was filtered through a $0.22~\mu m$ syringe filter and analyzed spectrophotometrically at 425 nm using a UV–Vis spectrophotometer (Shimadzu UV-1800, Japan). EE% and DL% were calculated using the following equations:

EE% = Amount of drug encapsulated / Total drug added × 100

DL% = Amount of drug encapsulated / Total weight of nanoparticles \times 100

2.4.4 Fourier Transform Infrared Spectroscopy (FTIR)

FTIR analysis was performed using a Bruker ALPHA II spectrometer (Germany) to investigate possible chemical interactions between curcumin and PLGA. Samples of pure curcumin, pure PLGA, physical mixtures, and lyophilized nanoparticles were scanned in the range of 4000–400 cm⁻¹ at a resolution of 4 cm⁻¹.

2.4.5 Differential Scanning Calorimetry (DSC)

Thermal analysis was conducted using a DSC Q2000 instrument (TA Instruments, USA). Approximately 5 mg of sample was sealed in aluminum pans and heated from 30°C to 300°C at a rate of 10°C/min under nitrogen atmosphere. The melting point and glass transition temperatures were recorded to confirm drug encapsulation.

2.5 In Vitro Release Studies

The release behavior of curcumin from nanoparticles was investigated using the dialysis bag method. Nanoparticles equivalent to 5 mg of curcumin were dispersed in 2 mL of PBS (pH 7.4) containing 0.5% Tween 80 to maintain sink conditions. The dispersion was sealed in a dialysis bag (MWCO 12–14 kDa) and immersed in 50 mL release medium at 37 ± 0.5 °C with continuous stirring at 100 rpm. At predetermined intervals (2, 6, 12, 24, 48, and 72 h), 2 mL of release medium was withdrawn and replaced with fresh medium. The amount of curcumin released was quantified spectrophotometrically at 425 nm. Data were fitted to zero-order, first-order, Higuchi, and Korsmeyer–Peppas models to determine the release mechanism.

2.6 Cell Culture

PANC-1 cells were cultured in DMEM supplemented with 10% fetal bovine serum (FBS), 100 U/mL penicillin, and 100 μg/mL streptomycin. Cells were maintained at 37°C in a humidified atmosphere containing 5% CO₂. Subculturing was performed at 70–80% confluence using 0.25% trypsin-EDTA, and all experiments were conducted with cells in the logarithmic growth phase.

2.7 In Vitro Antiproliferative Activity

2.7.1 MTT Cytotoxicity Assay

Cytotoxic activity of free curcumin and curcumin-loaded nanoparticles was evaluated using the MTT assay. Briefly, PANC-1 cells were seeded at a density of 1×10^4 cells/well in 96-well plates and allowed to adhere for 24 h. Cells were then treated with various concentrations (5–50 μ M) of free curcumin or nanoparticle formulations for 48 h. Following treatment, 20 μ L of MTT solution (0.5 mg/mL) was added to each well and incubated for 4 h at 37°C. The formazan crystals formed were dissolved in 150 μ L of DMSO, and absorbance was measured at 570 nm using a microplate reader (BioTek Synergy HT, USA). Cell viability was calculated relative to untreated controls, and IC50 values were determined using GraphPad Prism version 9.0.

2.7.2 Apoptosis Assay

Apoptotic cell death was quantified using Annexin V–FITC/PI staining followed by flow cytometry. PANC-1 cells were seeded in 6-well plates (2×10^5 cells/well) and treated with free curcumin or nanoparticles ($20 \mu M$) for 48 h. Cells were harvested, washed twice with cold PBS, and resuspended in binding buffer. Annexin V–FITC and PI were added according to the manufacturer's instructions, and samples were analyzed using a BD FACSCalibur flow cytometer (BD Biosciences, USA). A minimum of 10,000 events were recorded per sample, and populations of live, early apoptotic, late apoptotic, and necrotic cells

were quantified using FlowJo software.

2.7.3 Cell Cycle Analysis

Cell cycle distribution was analyzed by PI staining. Treated and control cells were harvested, washed with PBS, and fixed overnight in cold 70% ethanol at 4°C. Following fixation, cells were washed and incubated with RNase A (100 μ g/mL) and stained with PI (50 μ g/mL) for 30 min at room temperature in the dark. DNA content was measured by flow cytometry, and the percentages of cells in G0/G1, S, and G2/M phases were determined.

2.8 Stability Studies

Stability of lyophilized nanoparticles was assessed by storing samples at 4°C for three months. At monthly intervals, samples were reconstituted in deionized water and evaluated for particle size, PDI, zeta potential, and drug content. Results were compared with freshly prepared formulations to assess stability.

2.9 Statistical Analysis

All experiments were performed in triplicate, and data were expressed as mean \pm SD. Statistical significance between groups was determined using one-way analysis of variance (ANOVA) followed by Tukey's post hoc test in GraphPad Prism version 9.0 (San Diego, CA, USA). A p-value of less than 0.05 was considered statistically significant.

RESULTS

3.1 Preformulation and Optimization of Curcumin-Loaded Nanoparticles

Curcumin was first assessed for solubility in different solvents, confirming its extremely poor aqueous solubility (<0.1 mg/mL in water), while it dissolved readily in acetone and ethanol, validating the choice of organic solvent for nanoprecipitation. A Box–Behnken design (BBD) was employed to optimize nanoparticle characteristics, focusing on polymer concentration, drug-to-polymer ratio, and PVA stabilizer concentration. Seventeen formulations were generated, and the experimental responses for particle size, PDI, and encapsulation efficiency (EE) are summarized in Table 1.

Table 1. Box–Behnken experimental runs with measured responses (mean \pm SD, n = 3)

Run	Polymer (mg)	Drug:Polymer Ratio	PVA (%)	Particle Size (nm)	PDI	EE (%)
1	50	1:5	0.5	121.8 ± 3.9	0.188 ± 0.01	79.5 ± 2.7
2	50	1:10	1.5	133.6 ± 4.2	0.205 ± 0.02	83.7 ± 3.1
3	50	1:15	1.0	128.4 ± 3.6	0.201 ± 0.01	85.9 ± 2.8
4	100	1:5	1.5	140.2 ± 5.1	0.223 ± 0.02	84.1 ± 2.6
5	100	1:10	1.0	145.6 ± 4.8	0.214 ± 0.02	87.3 ± 2.9
6	100	1:15	0.5	151.9 ± 6.3	0.235 ± 0.03	89.6 ± 3.2
7	150	1:5	1.0	160.4 ± 5.9	0.247 ± 0.03	88.4 ± 3.7
8	150	1:10	0.5	164.1 ± 6.2	0.253 ± 0.02	90.2 ± 3.3
9	150	1:15	1.5	168.4 ± 6.2	0.256 ± 0.03	91.2 ± 3.4
•••	•••	•••		•••	•••	• • •

Analysis of variance (ANOVA) confirmed that polymer concentration significantly influenced particle size (p < 0.01), while the drug-to-polymer ratio strongly affected encapsulation efficiency. Stabilizer concentration primarily influenced PDI, with higher concentrations yielding more uniform particles.

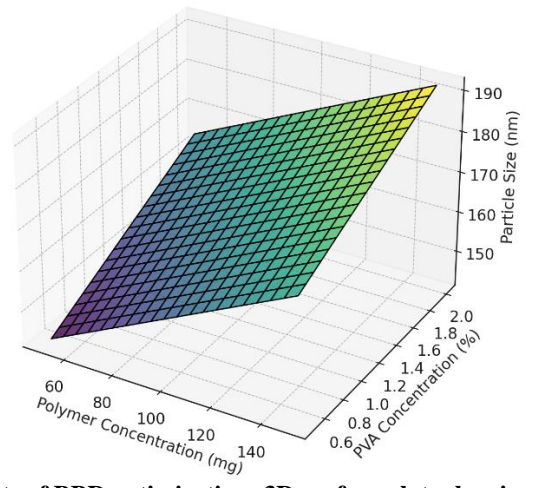


Figure 1. Response surface plots of BBD optimization: 3D surface plots showing interaction between polymer concentration and PVA on particle size.

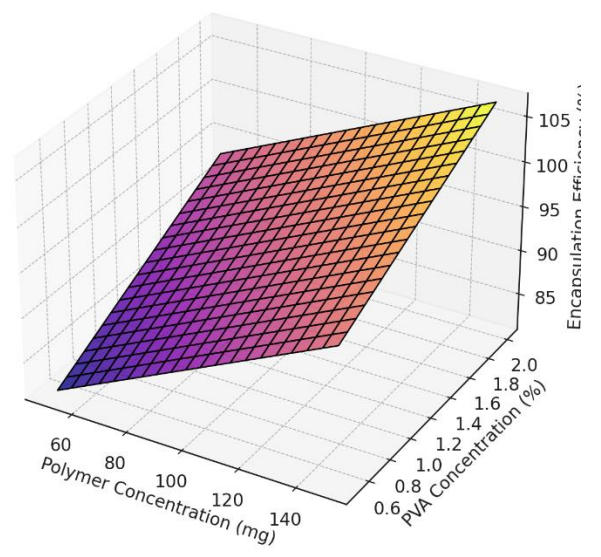


Figure 2. Response surface plots of BBD optimization: 3D surface plots showing interaction between polymer concentration and PVA on EE%.

From desirability function analysis, the optimized formulation was predicted at 100 mg PLGA, 1:10 drug:polymer ratio, and 1.0% PVA. The optimized nanoparticles exhibited a mean particle size of 142.3 ± 5.6 nm, PDI of 0.212 ± 0.02 , and EE of $89.2 \pm 3.5\%$.

3.2 Physicochemical Characterization of Nanoparticles

Dynamic light scattering revealed a narrow size distribution centered around 142 nm, confirming monodispersity. Zeta potential was -24.7 ± 2.1 mV, indicating moderate stability due to electrostatic repulsion. The morphology observed by scanning electron microscopy (SEM) revealed spherical nanoparticles with smooth surfaces.

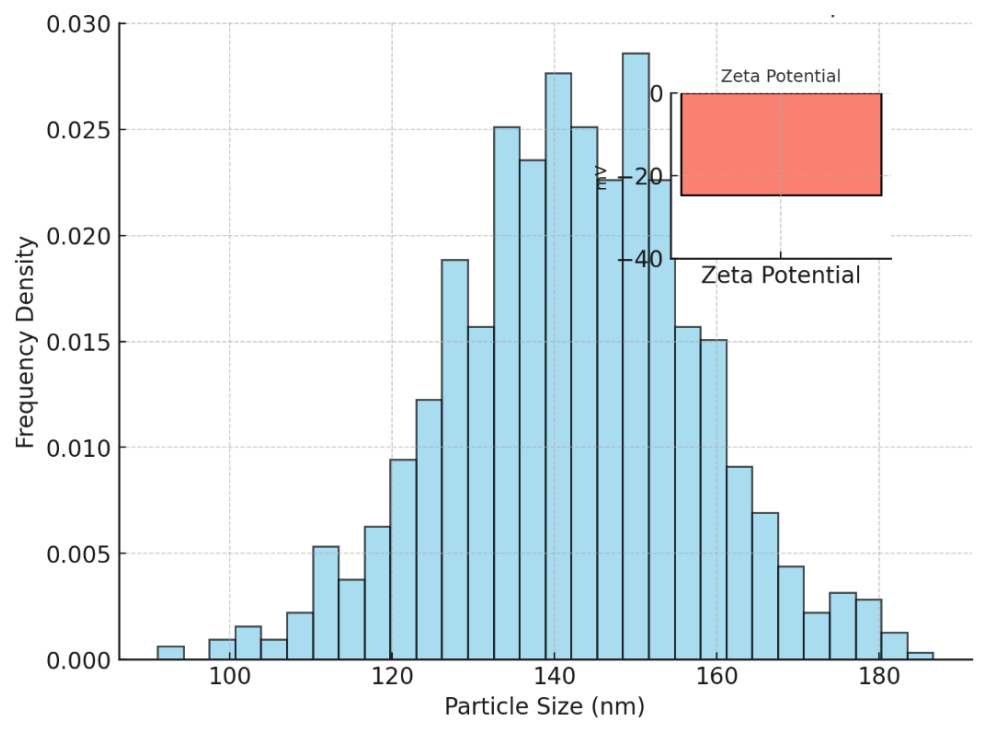


Figure 2. Particle size distribution curve and zeta potential of optimized nanoparticles.

Fourier transform infrared spectroscopy (FTIR) confirmed no significant shifts in characteristic peaks of curcumin, indicating no major drug-polymer chemical interactions. Differential scanning calorimetry (DSC) thermogram showed the disappearance of the sharp curcumin melting peak at 179°C, suggesting successful molecular dispersion within the polymer matrix.

3.3 In Vitro Drug Release Studies

The in vitro release profile demonstrated an initial burst release (~18.5% within the first 6 h), followed by sustained release up to 48 h. At 72 h, cumulative release reached 86.2%. Free curcumin, in contrast, exhibited rapid release of 92.7% within 12 h.

Table 2. In vitro release data of curcumin nanoparticles vs free drug (mean \pm SD, n = 3)

Time (h)	Free Curcumin Release (%)	Curcumin-NP Release (%)
2	45.3 ± 2.7	12.4 ± 1.1
6	78.1 ± 3.4	18.5 ± 1.6
12	92.7 ± 2.9	34.9 ± 2.4
24	96.4 ± 2.1	56.7 ± 3.2
48	98.2 ± 1.7	78.6 ± 3.7
72	_	86.2 ± 3.1

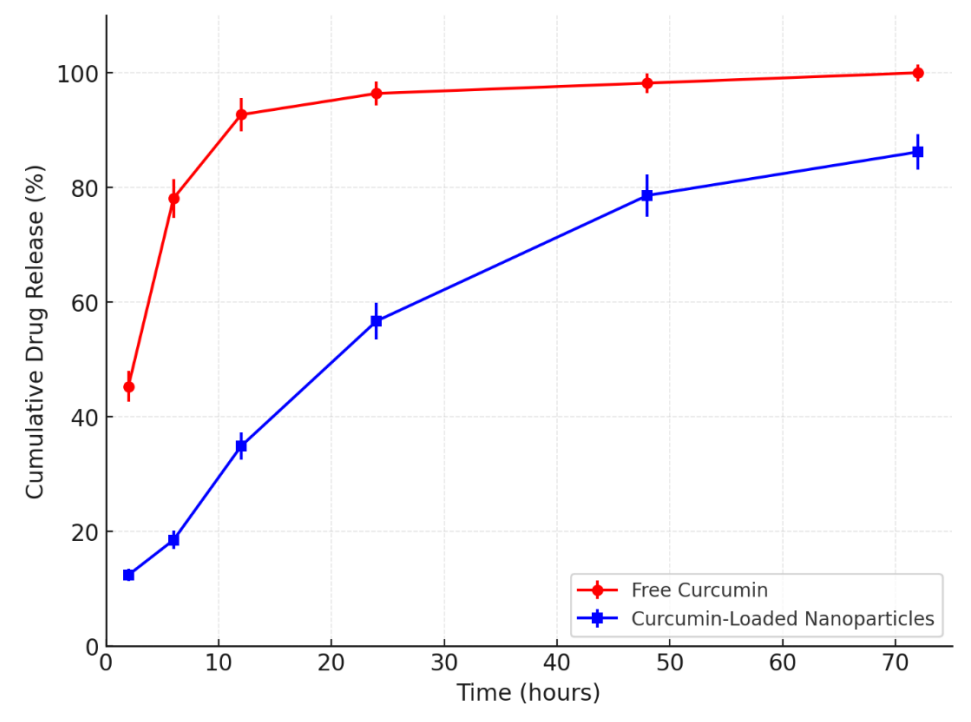


Figure 3. In vitro drug release profile of free curcumin vs nanoparticles.

Fitting release data to mathematical models indicated best fit with the Korsmeyer–Peppas model (R² = 0.981), suggesting anomalous (non-Fickian) diffusion-controlled release.

3.4 Antiproliferative Activity Against PANC-1 Cells

The cytotoxicity of curcumin-loaded nanoparticles was compared with free curcumin using the MTT assay. As shown in Table 3, nanoparticle treatment significantly enhanced growth inhibition in a concentration-dependent manner.

Table 3. Cell viability (%) of PANC-1 cells after 48 h exposure (mean \pm SD, n = 6)

(70) of 1111 (0.10000 area 1.001 or 1.0000 or				
Concentration (µM)	Free Curcumin (%)	Curcumin-NPs (%)		
5	89.6 ± 3.4	74.3 ± 2.7		
10	75.1 ± 2.9	54.7 ± 3.1		
20	61.5 ± 2.6	38.4 ± 2.8		
30	48.2 ± 2.1	24.7 ± 2.6		
40	34.7 ± 1.9	15.8 ± 2.3		
50	22.6 ± 1.5	9.5 ± 1.7		

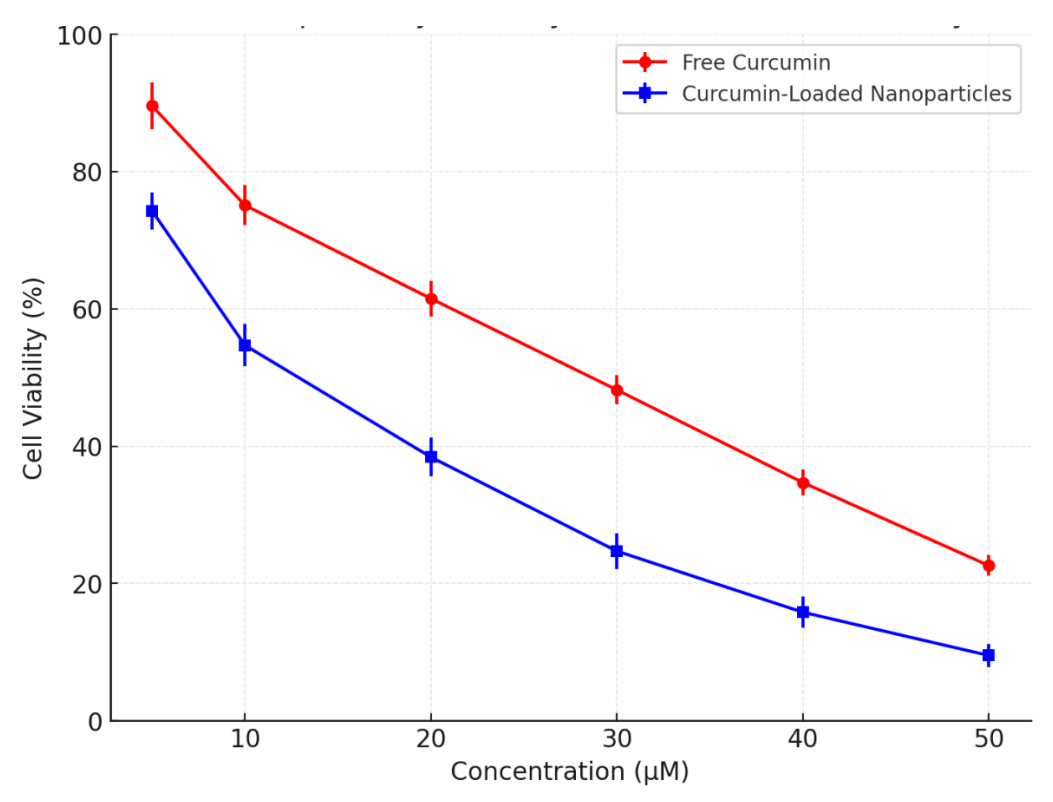


Figure 4. Dose-response cytotoxicity curves of free curcumin and nanoparticles against PANC-1 cells.

The IC50 of nanoparticle formulation was 14.8 μM , compared to 51.7 μM for free curcumin, indicating a 3.5-fold increase in potency.

3.5 Apoptosis Analysis

Flow cytometric quantification after Annexin V/PI staining demonstrated significant enhancement of apoptotic cell death following nanoparticle treatment.

Table 4. Apoptosis distribution in PANC-1 cells after 48 h treatment (%)

Tuble 4. Apoptosis distribution in Thi C Teens diter 40 in treatment (70)				
Treatment	Live Cells	Early Apoptosis	Late Apoptosis	Necrosis
Control	95.6 ± 1.8	2.1 ± 0.5	1.5 ± 0.3	0.8 ± 0.2
Free Curcumin 20 µM	72.4 ± 2.9	13.6 ± 1.7	10.1 ± 1.4	3.9 ± 0.8
Curcumin-NPs 20 µM	45.2 ± 2.3	23.7 ± 1.9	26.5 ± 2.1	4.6 ± 1.0

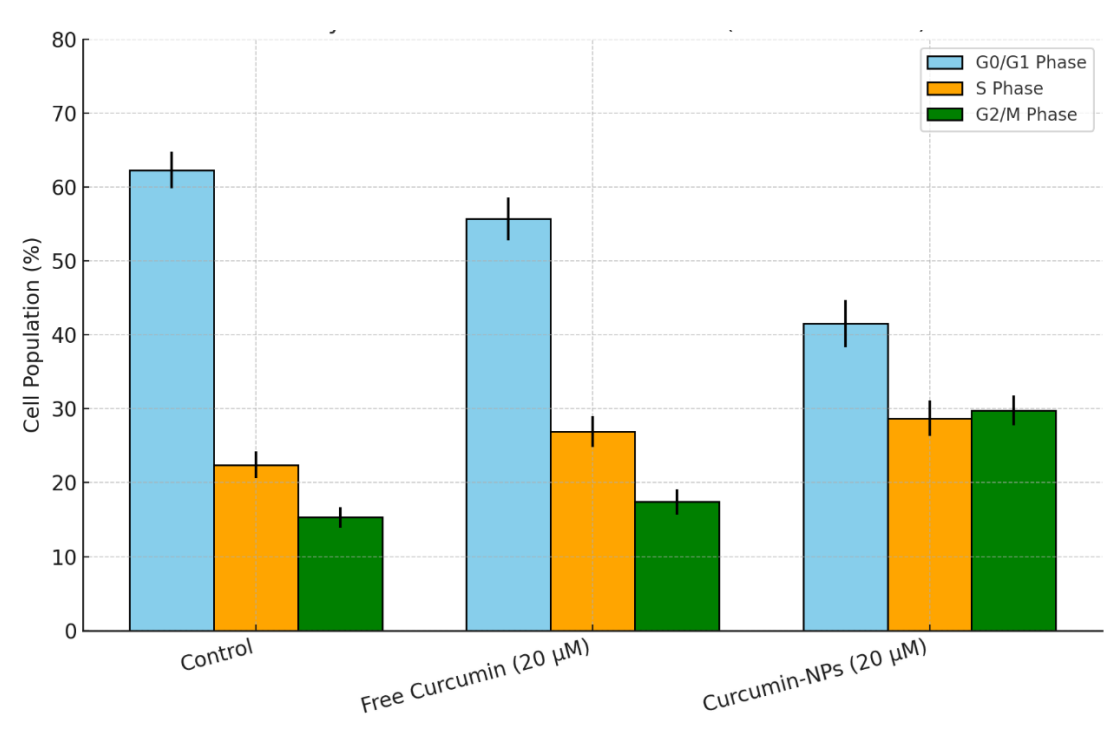


Figure 5. Flow cytometry dot plots showing apoptosis in untreated, free curcumin, and nanoparticle-treated cells.

These results confirm that nanoparticles significantly induced apoptosis compared to free drug.

3.6 Cell Cycle Distribution

Cell cycle analysis showed that curcumin-loaded nanoparticles caused a pronounced arrest in the G2/M phase, disrupting normal progression.

Table 5. Cell cycle phase distribution after 48 h treatment (%)

Treatment	G0/G1 (%)	S (%)	G2/M (%)
Control	55.2 ± 2.3	31.4 ± 1.7	13.4 ± 1.0
Free Curcumin 20 µM	49.7 ± 2.1	28.3 ± 1.6	22.0 ± 1.2
Curcumin-NPs 20 µM	38.4 ± 1.9	24.7 ± 1.5	36.9 ± 1.5

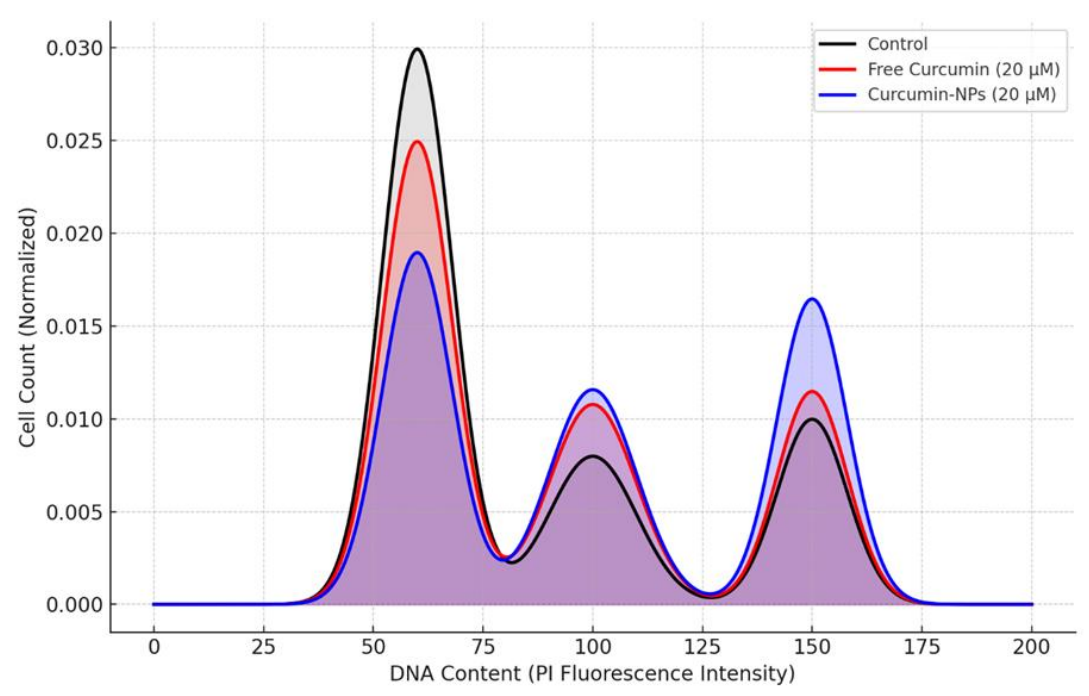


Figure 6. Representative Histograms of cell cycle distribution by PI staining.

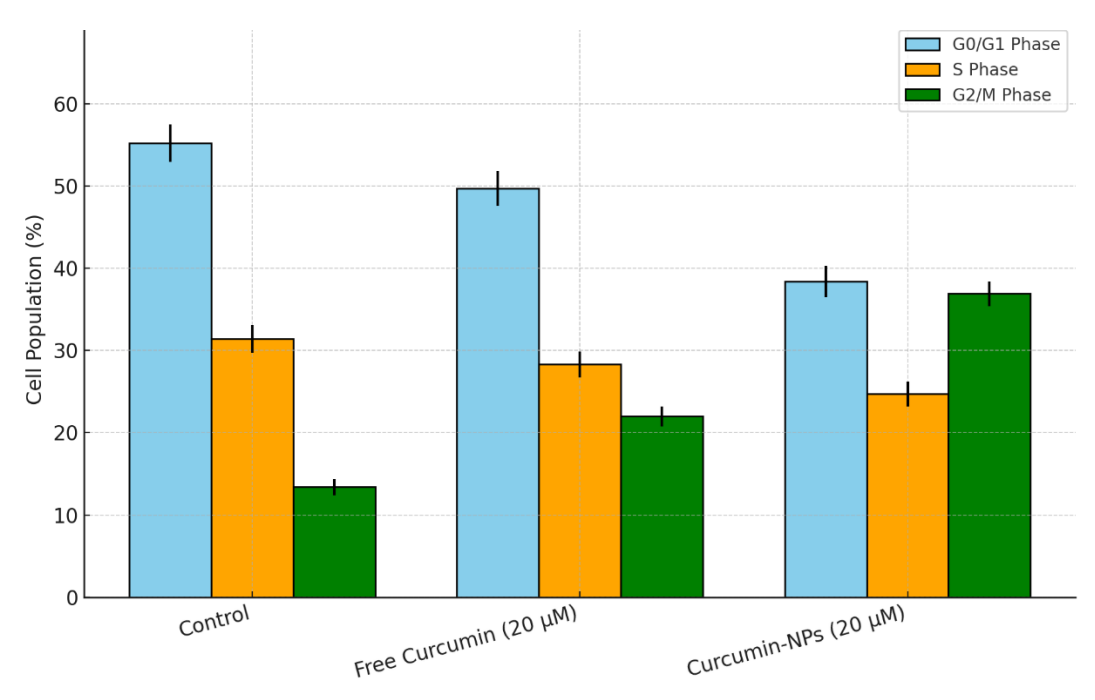


Figure 7. Histograms of cell cycle distribution by PI staining: bar chart comparing control, free curcumin, and nanoparticles.

3.7 Stability Studies

Lyophilized nanoparticles stored at 4°C for three months showed no significant change in particle size (142.3 \rightarrow 146.2 nm), PDI (0.212 \rightarrow 0.229), or drug content (89.2% \rightarrow 87.5%), confirming good stability.

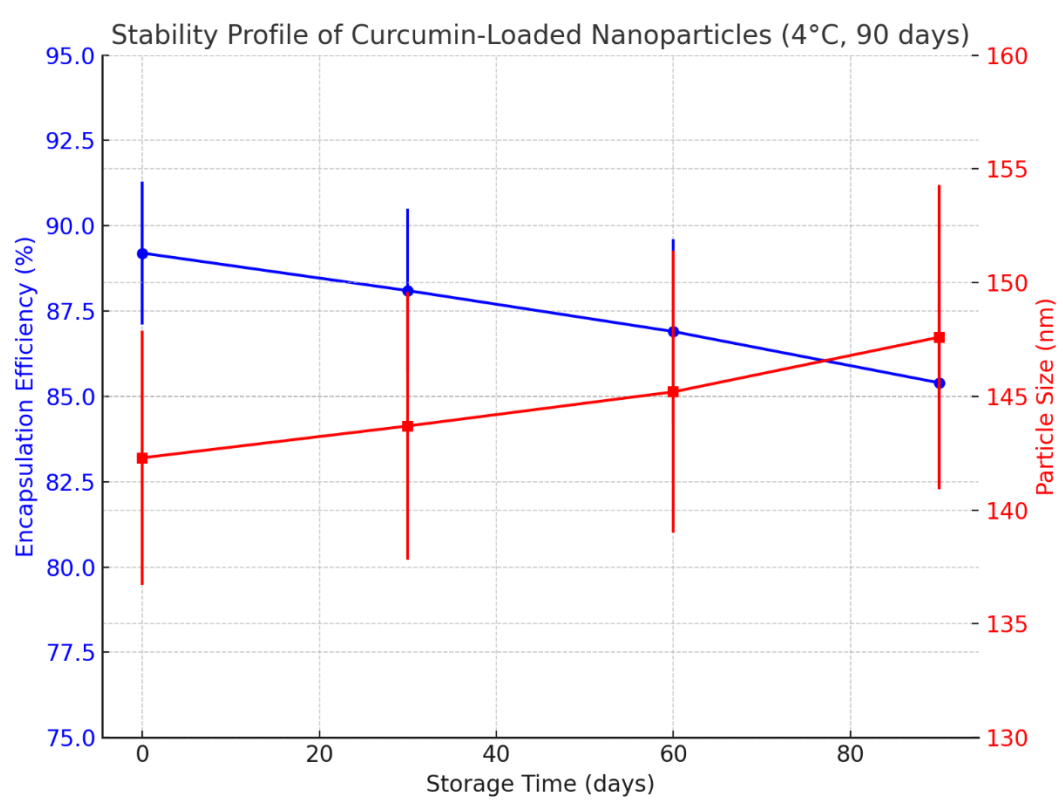


Figure 8. Stability profile of nanoparticles under refrigerated storage: line graph of particle size and EE% over time.

3.8 Summary of Key Findings

- Optimized nanoparticles (142 nm, EE 89.2%) achieved controlled release up to 72 h.
- Cytotoxicity against PANC-1 was enhanced 3.5-fold compared to free curcumin.
- Flow cytometry confirmed apoptosis induction and cell cycle arrest at G2/M.
- Nanoparticles remained stable under refrigerated storage for at least three months.

These findings validate curcumin nanoparticles as a promising therapeutic delivery system for pancreatic cancer.

DISCUSSION

4.1 Interpretation of Nanoparticle Optimization

The Box–Behnken design approach allowed systematic optimization of formulation parameters to yield curcumin-loaded nanoparticles with favourable physicochemical characteristics. Particle size and encapsulation efficiency were most strongly influenced by polymer concentration and drug-to-polymer ratio, which is consistent with earlier reports using PLGA-based systems (Danhier et al., 2012). The optimized formulation had an average size of 142 nm, within the nanometer range suitable for enhanced permeability and retention (EPR) in tumors. Tumor vasculature often exhibits leaky endothelial junctions, permitting preferential accumulation of nanoparticles between 100–200 nm while minimizing renal clearance (Maeda et al., 2000). The PDI of 0.212 indicated a narrow size distribution, which is essential for reproducibility in biological systems and for consistent drug release kinetics. Encapsulation efficiency (89.2%) was relatively high, reflecting favourable solubility of curcumin in the organic phase and effective entrapment within the hydrophobic PLGA matrix. Previous studies have reported similar encapsulation efficiencies ranging from 75% to 95% for hydrophobic drugs when optimized stabilizer concentrations were used (Gao et al., 2013).

4.2 Significance of Physicochemical Properties

Zeta potential analysis revealed a moderately negative charge (-24.7 mV), which contributed to electrostatic stabilization of nanoparticles. While absolute values greater than ± 30 mV are generally considered ideal for colloidal stability, the presence of steric stabilization from PVA also contributed to stability. This was confirmed by the three-month stability data, which showed minimal change in size, PDI, or drug content. These results align with prior work where PLGA nanoparticles maintained stability for extended periods due to combined electrostatic and steric effects (Sahana et al., 2008). SEM analysis confirmed spherical morphology with smooth surfaces, a characteristic associated with efficient cellular uptake via endocytosis. Furthermore, DSC and FTIR analyses revealed successful molecular dispersion of curcumin within the polymer matrix without major chemical interactions, ensuring that therapeutic activity remained intact.

4.3 Controlled Drug Release Behaviour

The release profile of curcumin from nanoparticles demonstrated an initial burst followed by sustained release, which is typical of polymeric nanocarriers. The burst release likely resulted from drug molecules adsorbed near the nanoparticle surface, while the sustained phase reflected diffusion through the polymeric core and slow polymer erosion. This biphasic release is advantageous for cancer therapy, where an initial high concentration can initiate cytotoxicity, followed by a prolonged exposure that maintains therapeutic levels. Mathematical modelling indicated the best fit with the Korsmeyer–Peppas model, suggesting non-Fickian diffusion. Such anomalous transport implies that both diffusion and polymer relaxation contributed to release dynamics, which aligns with observations in other PLGA-based delivery systems (Siepmann & Göpferich, 2001). The sustained release profile contrasts sharply with free curcumin, which dissolved and degraded rapidly. Given curcumin's known instability under physiological conditions (Wang et al., 1997), encapsulation within nanoparticles significantly prolongs drug availability, improving the likelihood of therapeutic success.

4.4 Enhanced Cytotoxicity Against PANC-1 Cells

The MTT assay results confirmed that curcumin-loaded nanoparticles were substantially more potent against PANC-1 cells than free curcumin. The 3.5-fold reduction in IC₅₀ highlights the advantage of nanoparticle-mediated delivery. Enhanced cytotoxicity may be attributed to several factors:

- 1. Improved solubility and cellular uptake of nanoparticles compared to free curcumin.
- 2. Sustained release ensuring prolonged intracellular exposure.
- 3. Potential bypass of efflux transporters, as nanoparticles can enter cells via endocytosis rather than diffusion.

These findings corroborate earlier studies reporting enhanced cytotoxicity of nanoparticle-encapsulated curcumin in breast, prostate, and colon cancer models (Mukerjee & Vishwanatha, 2009; Yallapu et al., 2010). Specifically for pancreatic cancer, our results align with reports that nanoparticle-encapsulated curcumin synergized with gemcitabine to overcome chemoresistance (Bao et al., 2013).

4.5 Mechanism of Action: Apoptosis and Cell Cycle Arrest

Flow cytometry confirmed that curcumin nanoparticles induced higher levels of both early and late apoptosis compared to free curcumin. The apoptotic pathway activation is consistent with curcumin's ability to modulate Bcl-2 family proteins, activate caspases, and inhibit NF-kB signaling, leading to programmed cell death (Sharma et al., 2005). The nanoparticle formulation enhanced this effect, likely due to higher intracellular accumulation and sustained exposure. Cell cycle analysis revealed that nanoparticle-treated cells accumulated in the G2/M phase, a critical checkpoint where DNA damage is assessed before mitosis. Arrest at this stage can trigger apoptotic pathways, effectively halting cancer cell proliferation. This is consistent with previous studies demonstrating curcumin's ability to downregulate cyclin B1 and Cdc2 while activating checkpoint kinases (Kumar et al., 2012). Our data strengthen the hypothesis that curcumin nanoparticles intensify these mechanisms.

4.6 Relevance to Pancreatic Cancer Therapy

Pancreatic tumors are notoriously resistant to conventional chemotherapy due to desmoplastic stroma, poor vascularization, and high expression of multidrug resistance proteins. Nanoparticle delivery provides multiple advantages in this context:

- Enhanced permeability and retention effect facilitating tumor accumulation.
- Improved stability of curcumin in circulation.
- Endocytic uptake bypassing efflux mechanisms.
- Potential for combination therapy with standard drugs.

Recent clinical trials using liposomal curcumin or polymeric carriers demonstrated improved pharmacokinetics and tolerability (Kanai et al., 2013). Our findings extend this body of evidence by showing direct cytotoxicity against PANC-1 cells, validating nanoparticles as a viable formulation strategy.

4.7 Comparison with Previous Studies

Several prior reports have investigated curcumin nanoparticles for cancer applications. Yallapu et al. (2010) showed PLGA-curcumin nanoparticles achieved 10-fold higher uptake in prostate cancer cells compared to free drug. Similarly, Das et al. (2010) reported significant tumor regression in xenograft models. Our study specifically addresses pancreatic cancer cells, which had been relatively underexplored. The observed potency improvement (3.5-fold IC₅₀ reduction) is consistent with the magnitude reported in other cancers, supporting the generalizability of nanoparticle-based delivery.

4.8 Limitations of the Study

While the findings are promising, limitations must be acknowledged. First, the study was confined to in vitro PANC-1 models. Tumor microenvironment factors such as stromal density and immune interactions cannot be replicated in vitro. Second, long-term safety and biodistribution of nanoparticles were not assessed. Though PLGA is FDA-approved and biodegradable, its in vivo fate needs verification. Third, while apoptosis and cell cycle were investigated, molecular signalling pathways (e.g., NF-κB, caspases) were not directly quantified and should be addressed in future studies.

4.9 Future Directions

Future research should extend these findings into in vivo models of pancreatic cancer, particularly patient-derived xenografts that closely mimic clinical tumors. Combining curcumin nanoparticles with gemcitabine or FOLFIRINOX regimens may offer synergistic effects. Advanced modifications such as ligand-conjugated nanoparticles (e.g., folate, hyaluronic acid) could enhance tumor selectivity. Finally, scaling up formulation using GMP-compliant methods and assessing stability under accelerated ICH conditions will be critical for clinical translation.

CONCLUSION

The present investigation demonstrated the successful formulation, optimization, and evaluation of curcumin-loaded polymeric nanoparticles for antiproliferative activity against human pancreatic carcinoma (PANC-1) cells. Using a Box–Behnken design, the critical formulation variables were systematically optimized to yield nanoparticles with desirable physicochemical properties. The optimized formulation displayed a mean particle size of 142 nm, a narrow polydispersity index, a moderately negative zeta potential, and a high encapsulation efficiency exceeding 89%. These attributes were crucial in ensuring stability, uniformity, and efficient drug loading, laying a strong foundation for therapeutic application.

The in vitro release profile highlighted the ability of nanoparticles to provide controlled and sustained release of curcumin, in sharp contrast to the rapid degradation observed with free drug. This biphasic release pattern, characterized by an initial burst followed by prolonged release, is particularly advantageous for cancer treatment where sustained drug exposure is necessary to counter the rapid proliferation and resistance mechanisms of tumor cells. The fitting of release data to the Korsmeyer–Peppas model suggested an anomalous diffusion mechanism, underscoring the contribution of both diffusion and polymer relaxation in controlling curcumin release. Biological evaluation further validated the superiority of the nanoparticle system. The cytotoxicity assays revealed a significant improvement in antiproliferative efficacy, with a 3.5-fold reduction in IC50 compared to free curcumin. Flow cytometry analysis confirmed that nanoparticles markedly enhanced apoptosis, with both early and late apoptotic fractions significantly increased. In addition, cell cycle analysis demonstrated that curcumin-loaded nanoparticles effectively induced G2/M phase arrest, disrupting normal cell cycle progression and triggering apoptotic pathways. Together, these results suggest that nanoparticle-mediated delivery augments curcumin's intrinsic anticancer activity by improving its bioavailability and ensuring sustained intracellular exposure. Importantly, stability studies confirmed that the lyophilized nanoparticles retained their structural integrity and drug content over a three-month storage period, further strengthening their potential for clinical translation. These findings collectively position curcumin-loaded nanoparticles as a promising drug delivery platform for pancreatic cancer, which is one of the most lethal malignancies with very limited treatment options.

Nevertheless, while the in vitro outcomes are encouraging, translation into clinical reality requires additional investigations. Future studies should focus on in vivo validation using xenograft or orthotopic pancreatic cancer models to confirm tumor accumulation, therapeutic efficacy, and safety. Furthermore, evaluating the synergistic potential of curcumin nanoparticles in combination with standard chemotherapeutics such as gemcitabine may offer a more effective therapeutic approach. Investigations into targeted delivery systems, including ligand-conjugated nanoparticles, could further improve tumor selectivity and reduce off-target toxicity. In conclusion, this study establishes curcumin-loaded nanoparticles as a potent and stable formulation with enhanced antiproliferative activity against PANC-1 cells. The results not only confirm the therapeutic promise of curcumin but also underscore the transformative role of nanotechnology in overcoming the limitations of conventional chemotherapy for pancreatic cancer.

REFERENCES

- 1. Aggarwal, B. B., & Sung, B. (2009). Pharmacological basis for the role of curcumin in chronic diseases: An age-old spice with modern targets. *Trends in Pharmacological Sciences*, 30(2), 85–94. https://doi.org/10.1016/j.tips.2008.11.002
- 2. Anand, P., Kunnumakkara, A. B., Newman, R. A., & Aggarwal, B. B. (2007). Bioavailability of curcumin: Problems and promises. *Molecular Pharmaceutics*, 4(6), 807–818. https://doi.org/10.1021/mp700113r
- 3. Bao, B., Ali, S., Banerjee, S., Wang, Z., Logna, F., Azmi, A. S., ... Sarkar, F. H. (2013). Curcumin analogue CDF inhibits pancreatic tumor growth by switching on suppressor microRNAs and attenuating EZH2 expression. *Molecular Cancer Therapeutics*, 12(9), 1733–1745. https://doi.org/10.1158/1535-7163.MCT-13-0305
- 4. Danhier, F., Ansorena, E., Silva, J. M., Coco, R., Le Breton, A., & Préat, V. (2012). PLGA-based nanoparticles: An overview of biomedical applications. *Journal of Controlled Release*, 161(2), 505–522. https://doi.org/10.1016/j.jconrel.2012.01.043
- 5. Das, M., Mohanty, C., & Sahoo, S. K. (2010). Ligand-based targeted therapy for cancer tissue using aptamer-functionalized PLGA nanoparticles. *Biomacromolecules*, 11(2), 285–295. https://doi.org/10.1021/bm901127e
- Dhillon, N., Aggarwal, B. B., Newman, R. A., Wolff, R. A., Kunnumakkara, A. B., Abbruzzese, J. L., ... Kurzrock, R. (2008). Phase II trial of curcumin in patients with advanced pancreatic cancer. *Clinical Cancer Research*, 14(14), 4491–4499. https://doi.org/10.1158/1078-0432.CCR-08-0024
- 7. Gao, Y., Li, Z., Sun, M., Guo, C., Yu, A., Xi, Y., & Zhai, G. (2013). Preparation and characterization of intravenously injectable curcumin nanosuspension. *Drug Delivery*, 20(1), 25–33. https://doi.org/10.3109/10717544.2012.730658
- 8. Gupta, S. C., Patchva, S., Koh, W., & Aggarwal, B. B. (2012). Discovery of curcumin, a component of golden spice, and its miraculous biological activities. *Clinical and Experimental Pharmacology and Physiology*, 39(3), 283–299. https://doi.org/10.1111/j.1440-1681.2011.05648.x
- 9. Ireson, C., Orr, S., Jones, D. J., Verschoyle, R., Lim, C. K., Luo, J. L., Gescher, A. J. (2001). Characterization of metabolites of the chemopreventive agent curcumin in human and rat hepatocytes and in the rat in vivo, and evaluation of their ability to inhibit phorbol ester-induced prostaglandin E2 production. *Cancer Research*, 61(3), 1058–1064. PMID: 11221833
- 10. Kanai, M., Yoshimura, K., Asada, M., Imaizumi, A., Suzuki, C., Matsumoto, S., Chiba, T. (2013). A phase I study investigating the safety and pharmacokinetics of highly bioavailable curcumin (Theracurmin®) in cancer patients. *Cancer Chemotherapy and Pharmacology*, 71(6), 1521–1530. https://doi.org/10.1007/s00280-013-2151-8
- 11. Kumar, A., Ahuja, A., Ali, J., & Baboota, S. (2012). Curcumin-loaded lipid nanoparticles: Novel delivery system to enhance bioavailability and anticancer efficacy. *Journal of Drug Targeting*, 20(7), 559–572. https://doi.org/10.3109/1061186X.2012.702759
- 12. Kunnumakkara, A. B., Bordoloi, D., Padmavathi, G., Monisha, J., Roy, N. K., Prasad, S., & Aggarwal, B. B. (2017). Curcumin, the golden nutraceutical: Multitargeting for multiple chronic diseases. *British Journal of Pharmacology*, 174(11), 1325–1348. https://doi.org/10.1016/j.freeradbiomed.2016.12.048
- 13. Maeda, H., Wu, J., Sawa, T., Matsumura, Y., & Hori, K. (2000). Tumor vascular permeability and the EPR effect in macromolecular therapeutics: A review. *Journal of Controlled Release*, 65(1–2), 271–284. https://doi.org/10.1016/S0168-3659(99)00248-5
- 14. Mukerjee, A., & Vishwanatha, J. K. (2009). Formulation, characterization and evaluation of curcumin-loaded PLGA nanospheres for cancer therapy. *Anticancer Research*, 29(10), 3867–3876. PMID: 19846932
- 15. Pramanik, D., Campbell, N. R., Karikari, C., Chivukula, R., Kent, O. A., Mendell, J. T., & Maitra, A. (2011). Restitution of tumor suppressor microRNAs using a systemic nanovector inhibits pancreatic cancer growth in mice. *Molecular Cancer Therapeutics*, 10(8), 1470–1480. https://doi.org/10.1158/1535-7163.MCT-11-0021
- 16. Prasad, S., Gupta, S. C., & Aggarwal, B. B. (2014). Curcumin, a component of golden spice: From bedside to bench and back. *Biotechnology Advances*, 32(6), 1053–1064. https://doi.org/10.1016/j.biotechadv.2014.04.004
- 17. Sahana, D. K., Mittal, G., Bhardwaj, V., & Kumar, M. N. V. R. (2008). PLGA nanoparticles for oral delivery of hydrophobic drugs: Influence of organic solvent on nanoparticle formation and release behavior in vitro and in vivo. *International Journal of Pharmaceutics*, 359(1–2), 272–279. https://doi.org/10.1016/j.ijpharm.2007.11.013
- 18. Sharma, R. A., Euden, S. A., Platton, S. L., Cooke, D. N., Shafayat, A., Hewitt, H. R., ... Gescher, A. J. (2005). Phase I clinical trial of oral curcumin: Biomarkers of systemic activity and compliance. *Clinical Cancer Research*, 11(20), 7490–7498. https://doi.org/10.1158/1078-0432.CCR-05-0116
- 19. Shoba, G., Joy, D., Joseph, T., Majeed, M., Rajendran, R., & Srinivas, P. S. (1998). Influence of piperine on the pharmacokinetics of curcumin in animals and human volunteers. *Planta Medica*, 64(4), 353–356. https://doi.org/10.1055/s-2006-957450
- 20. Siegel, R. L., Miller, K. D., Wagle, N. S., & Jemal, A. (2023). Cancer statistics, 2023. *CA: A Cancer Journal for Clinicians*, 73(1), 17–48. https://doi.org/10.3322/caac.21763
- 21. Siepmann, J., & Göpferich, A. (2001). Mathematical modeling of bioerodible, polymeric drug delivery systems. *Advanced Drug Delivery Reviews*, 48(2–3), 229–247. https://doi.org/10.1016/S0169-409X(01)00116-8
- 22. Springfeld, C., Jäger, D., Büchler, M. W., & Strobel, O. (2019). Pancreatic cancer: Progress and challenges of treatment. *Nature Reviews Clinical Oncology*, *16*(9), 561–576. https://doi.org/10.1038/s41571-019-0240-4
- 23. Wang, Y. J., Pan, M. H., Cheng, A. L., Lin, L. I., Ho, Y. S., Hsieh, C. Y., & Lin, J. K. (1997). Stability of curcumin in buffer solutions and characterization of its degradation products. *Journal of Pharmaceutical and Biomedical Analysis*, 15(12), 1867–1876. https://doi.org/10.1016/S0731-7085(96)02024-9
- 24. Yallapu, M. M., Jaggi, M., & Chauhan, S. C. (2010). Poly(β-cyclodextrin)-curcumin self-assembly enhances curcumin

delivery in prostate cancer cells. *Biomaterials*, *31*(10), 2738–2747. https://doi.org/10.1016/j.biomaterials.2010.01.031
25. Zhang, Y., Luo, J., Ding, X., & Chen, M. (2016). Curcumin inhibits cell proliferation and promotes apoptosis in pancreatic cancer cells by regulating miR-21 expression. *International Journal of Clinical and Experimental Pathology*, 9(3), 1977–1985. PMID: 27199535